Arch Orthop. 2026;6(1):1–11.

Archives of Orthopaedics Original Research

Development of a Novel Model of Pseudarthrosis in Rabbits: Low Expression of RUNX2 and COL1A1 Genes During Fracture Healing

Achraf Lajmi[1], Raja Amri[2,*], Ameny Chelly[3], Melek Turki[1], Nizar Sahnoun[1], Hassib keskes[1,2]

[1]Department of Orthopedic Surgery and Traumatology, Habib Bourguiba University Hospital, Sfax, Tunisia

[2]Research Laboratory Cell Therapy and Experimental Musculoskeletal System, Faculty of Medicine, Sfax, Tunisia

[3]Laboratory of Molecular and Cellular Screening Processes, Centre of Biotechnology of Sfax, Sfax, Tunisia

[*]Correspondence should be addressed to Raja Amri, raja.amri89@hotmail.fr

Received date: October 27, 2025, **Accepted date:** February 17, 2026

Citation: Lajmi A, Amri R, Chelly A, Turki M, Sahnoun N, Keskes H. Development of a Novel Model of Pseudarthrosis in Rabbits: Low Expression of RUNX2 and COL1A1 Genes During Fracture Healing. Arch Orthop. 2026;6(1):1–11.

Abstract

Aims: The present study investigated Runt-related transcription factor 2 (*RUNX2*) and collagen type A1 (*COL1A1*) gene expressions in pseudarthrosis with the objective of creating a novel shaft femoral pseudarthrosis rabbit model.

Methods: Sixteen rabbits were used in this experimental study. We divided rabbits into two groups, control group and pseudarthrosis group. The study aimed to compare bone consolidation between two groups: a control group, where a resection site was created and stabilized using an external fixator on both sides, and the pseudarthrosis (PS) group, where a muscle interposition was performed at the resection site in addition to the external fixation. At eight weeks, radiographic and molecular studies were undertaken to investigate bone consolidation in the resection area. We used Quantitative Polymerase Chain Reaction (Q-PCR) to evaluate the expression of the *RUNX2* and *COL 1A1* genes.

Results: In the control group, complete bone consolidation was achieved in all rabbits, as evidenced by macroscopic and radiographic assessments showing cortical continuity, a homogeneous medullary cavity, and the formation of a mature, continuous callus with clear cortico-medullary differentiation. In contrast, all animals in the PS group exhibited failed bone healing, characterized by the absence of cortical bridging and the presence of a persistent inter-fragmentary gap, medullary canal obliteration, and resorption of bone ends. At the molecular level, quantitative PCR analysis revealed significantly higher expression of *RUNX2* and *COL1A1* in the control group compared to the PS group ($p = 0.01$), with both genes demonstrating a 10-fold upregulation, reflecting increased osteogenic activity associated with successful bone regeneration.

Conclusion: We successfully established a rabbit model of femoral shaft pseudarthrosis, confirmed through the analysis of *COL1A1* and *RUNX2* gene expression levels.

Keywords: Pseudarthrosis, *RUNX2*, *COL1A1*, Rabbits

Introduction

Pseudarthrosis (PSA) is defined as a lack of radiographic consolidation six months after a traumatic incident, which is connected with the need for revision surgery. According to the Food and Drug Administration (FDA), PSA is diagnosed at least nine months after the incident, with no obvious signs of progressive healing for three months [1,2].

An increased incidence of pseudarthrosis in femoral shaft fractures has recently been observed due to the increased survival of patients with multiple severe injuries and the widening of indications for intramedullary nailing [3]. A recent study confirmed that [4], the overall non-union rate has been higher in the tibia and in the femur, compared to the humerus. Moreover, Ekegren *et al.* designed a large study using the Victorian Orthopedic Trauma Outcomes Registry of Australia to determine the rate of failure of long bone fractures and, according to the type of bone fracture, 2.3% of failures were found in the proximal humerus, 7.8% in the humerus shaft, 4.2% in the subtrochanteric fracture, 13.5% in the femur shaft, 8.4% in the distal femur, and 11.7% in the tibia shaft [5].

The non-consolidation of femur fracture causes pain, especially during loading, increased and abnormal mobility at the fracture site, functional limitations of the contiguous joints and muscle hypotrophy [6]. It represents a major challenge for orthopedic surgeons, and current therapeutic methods remain inadequate. It is often associated with reduced bone quality and can, therefore, adversely affect quality of life. Numerous surgical approaches for the treatment of pseudarthrosis were mentioned in the literature, such as electromagnetic fields [7]; low-intensity ultrasound [8], extracorporeal shock wave therapy (ESWT) [9], external fixators [10] and osteosynthesis with plate and screws [11]. Moreover, several studies have reported positive results after the treatment of non-union of the femur with single or double plate fixation combined with autologous bone graft [12,13]. Despite the progress in surgical methods and the development of novel implants, treatment of bone nonunion remains a challenge for orthopedic surgeons. Extended therapy, which can last months or even years, is expensive and adversely affects the patients' professional and personal life [14,15].

To minimize complications, successful revision surgery for pseudarthrosis often requires a surgical approach that is different from the first, further instrumentation, and other materials such as bone grafts or biologics. For this purpose, in our study, we are planning to create a novel model of pseudarthrosis in a small animal for further *in vivo* and *in vitro* research, aimed finally as a foundation in research to study the bone healing process and at identifying the most suitable treatment technique for pseudarthrosis.

The development of appropriate models of pseudarthrosis in animals will improve the knowledge of therapeutic procedures and allow the assessment of a variety of new surgical techniques for obtaining more effective and objective results. In the literature, several preclinical *in vivo* animal models of PSA have succeeded in creating a model of pseudarthrosis in rats, extensive resection of the periosteum and bone marrow is important for a reproducible model of atrophic pseudarthrosis in a rat femur [16]. Others have created a rat model of tibia fracture [17].

Rabbit models for spinal and tibial pseudarthrosis have been well-documented in the literature [18]. However, there is no robust evidence on which biological approach is more reliable for creating femoral shaft pseudarthrosis. Therefore, in our study, we suggest for the first time an approach of creating PS using muscle interposition technique in rabbits. This approach involves creating a bone defect in the femoral shaft of a rabbit, interposing the tensor fascia lata (TFL) muscle at the defect site, and stabilizing the construct with an external fixator. Radiographic and macroscopic assessments were realized at 8 weeks post-animal model establishment. Interestingly, we also validated the success of our technique through molecular quantification of bone consolidation markers *RUNX2* and *COL1A1*.

Runx2/Cbfa1 is a pivotal transcription factor essential for bone consolidation and skeletal development. It serves as a master regulator of bone formation and repair by orchestrating the differentiation, maturation, and functional activity of osteoblasts and chondrocytes throughout the consolidation process [19]. Moreover, *COL1A1* is fundamental to bone structure and function. It not only provides the framework for mineralization but also plays a dynamic role in bone growth, remodeling, and repair. Its integrity is vital for skeletal health, and disruptions in its expression or structure can lead to severe bone disorders [20].

Materials and Methods

Animal groups

Sixteen healthy adult New Zealand white rabbits of 7 to 8 months of age were used in this study (with an average body weight of 2.5 ± 0.09 kg). They were housed in individual cages. All animals were allowed free access to food and water under a temperature-controlled environment (25 ± 2°C) with regular 12:12h light-dark cycle. Rabbits were also given an acclimatization period of 10 days before initiation of our research. Rabbits were randomly divided into two groups, including one control group and one experimental group of PSA (group G1). The principle was to perform a 10 mm bone resection in femur protected by an external fixator with 2 plugs on both sides of the fracture in order to maintain the alignment of both extremities in both groups. In the second group, representing pseudarthrosis, muscle interposition was performed at the resection site. Bone consolidation was then evaluated at 8 weeks in both groups. In our model, pseudarthrosis was defined as the absence of bone healing after 8 weeks. The choice of this 8-week period was based on the time required for complete bone healing in rabbits, as reported in the literature [21].

Ethical statement

All experimental procedures were approved by the Ethics Committee of the Laboratory of Targeted Therapy and Animal Experimentation, Faculty of Medicine, Sfax, Tunisia (Protocol No.21/2023). The study was conducted in strict accordance with international guidelines for the care and use of laboratory animals and adhered to the principles of the 3Rs (Replacement, Reduction, and Refinement). All efforts were made to minimize animal suffering. Surgical procedures were performed under general anesthesia using ketamine (35–50 mg/kg) and xylazine (5–10 mg/kg, IM), with additional local anesthesia when needed. Postoperative analgesia was provided using buprenorphine (0.05–0.1 mg/kg, SC, every 8–12 h) and/or meloxicam (0.1–0.2 mg/kg, SC, for 2–3 days).

Animals were monitored daily for signs of distress, changes in behavior, appetite, or locomotion. At the end of the study, animals were euthanized humanely following approved institutional protocols.

Establishment of a rabbit PSA model

After anesthesia, the anterolateral aspect of the thigh was shaved, and the limb was washed with physiological saline. Brushing was done aseptically with Betadine®, and then the limb was covered with a sterile field with holes leaving the shaved area exposed (**Figure 1A**). After that, the skin incision was made on the anterolateral aspect of the thigh along the femur, sparing the adjacent proximal and distal joints (approximately 4 cm) (**Figure 1B**).

For the control group, in order to expose the femur, a dissection was performed through the aponeurosis, which is situated between the muscles of the anterior and posterior compartments of the thigh, straight up to the bone (**Figure 1C**).

After this, two 1.6 mm diameter pins were symmetrically placed on either side of the resection area using an orthopedic motor, and a mini external fixator was installed on the four pins. A bone resection of 10 mm was carried out using an electric micro-saw, followed by irrigation with saline solution. The alignment of the four pins, and consequently the two bone ends on either side of the fracture site, was verified. Finally, the stability of the external fixator and pins was checked using a screwdriver (**Figure 1D**). The procedure ensured proper stabilization and alignment of the bone fragments for optimal healing conditions.

For the PS group, after placement of the external fixator, a bone resection was performed. The TFL was identified at the level of the anterior surface of the thigh. It was resected partially at the level of its distal insertion opposite the patella and was reattached with a non-absorbable suture (**Figure 2A**). Subsequently, we proceeded with a dissection through the aponeurosis located between the muscles of the anterior compartment and those of the posterior compartment of the thigh to the bone to expose the femur. Then, we created a passage of the TFL between the muscles of the anterior compartment of the thigh and its interposition in the already prepared fracture site. The thickness of the interposed TFL occupied the entire resection zone in all cases (10 mm).

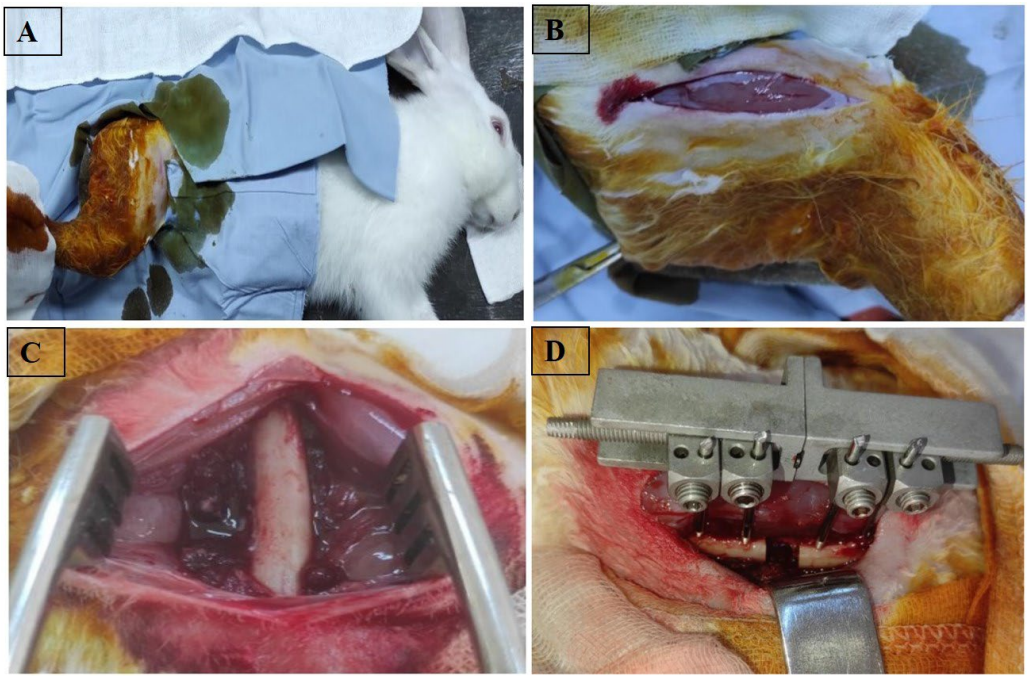

Figure 1. A) Sterile disinfection of the limb after shaving using Betadine®, followed by placement of a sterile drape exposing the shaved area; **B**) Skin incision made on the anterolateral aspect of the thigh along the femur, sparing the proximal and distal joints (approximately 4 cm), **C**) Exposure of the femur in the control group by dissection through the aponeurosis between the anterior and posterior thigh muscles, reaching the bone; **D**) Installation of a mini external fixator after symmetrical placement of two 1.6 mm diameter pins on each side of the resection site, followed by a 10 mm bone resection and verification of alignment and stability.

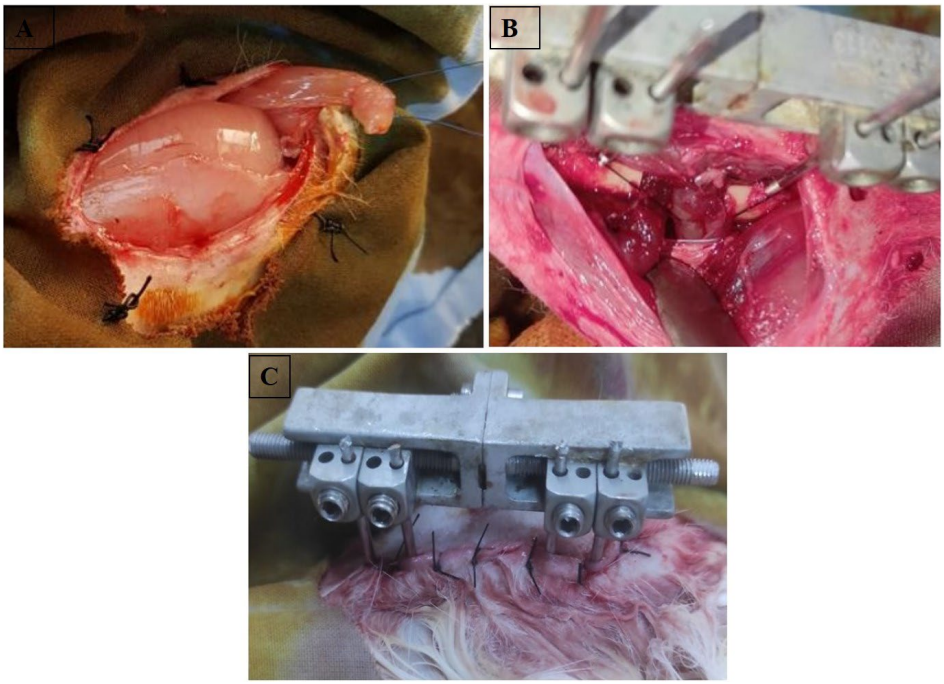

Figure 2. A) TFL identification marked with a non-absorbable suture (TFL = Tensor Fasciae Latae), **B**) Interposition of the TFL between the anterior thigh muscles and placement within the fracture site, then fixation to the posterior compartment muscles using an X-shaped suture reinforced with two half-overlocks and an additional non-absorbable suture passed in a figure-eight configuration around the four pins; **C**) Final wound closure after irrigation with sterile saline and suturing of the muscle and skin layers using 3-0 nylon (Ethilon, Ethicon, Norderstedt, Germany).

The TFL was fixed in the muscles of the posterior compartment of the thigh by an X-shaped point reinforced by two half-overlocks. Then, reinforcement of the fixation of the TFL by a point using a non-absorbable wire which passes through the 4 pins in 8 and housing the TFL on either side of the bone (**Figure 2B**). Finally, the wound was irrigated with sterile saline. The muscle and skin were afterward sutured back over with 3-0 nylon (Ethilon, Ethicon, Norderstedt, Germany) (**Figure 2C**).

In the postoperative period, the rabbits were given tramadol HCl® Ampule (Teriak, Zaghouan, Tunisia) (10 mg/kg) intramuscularly, every 24 hours for three days. They were also given daily cleanings of the surgical site with 0.9% NaCl solution for ten days. The sutures were removed thereafter.

Rabbits were sacrificed after 8 weeks (for the control and P1 groups) and the specimens were conserved at -80°.

Euthanasia and Sample preparation

Euthanasia was carried out by sectioning the two jugular veins at the neck. The resection was performed by cutting between the two pins located on either side of the target area, initially preserving the external fixator. The resected area, including the surrounding soft tissue, was removed in one piece (**Figure 3A**). This block was then divided longitudinally into two fragments (**Figure 3B**). Subsequently, the external fixator and its pins were removed. One of the fragments was allocated for molecular biology analysis.

Macroscopic study

A careful visual inspection of the samples was performed after fixation. The macroscopic factors evaluated in our study included cortical continuity, the appearance of the bone ends, the characteristics of the tissue occupying the bone resection area and its consistency, and the presence of deformity.

Radiographic evaluation: volumetric imaging by conical beam: the « cone beam »

The lower limbs were transported for a radiological study based on cone-beam volumetric imaging. All samples were placed on a plate after numbering, and a metallic marker was positioned in one corner of the plate for identification. The evaluation of the bone callus using cone-beam volumetric imaging was performed through the analysis of axial, frontal, and coronal slices, as well as 3D reconstruction. The

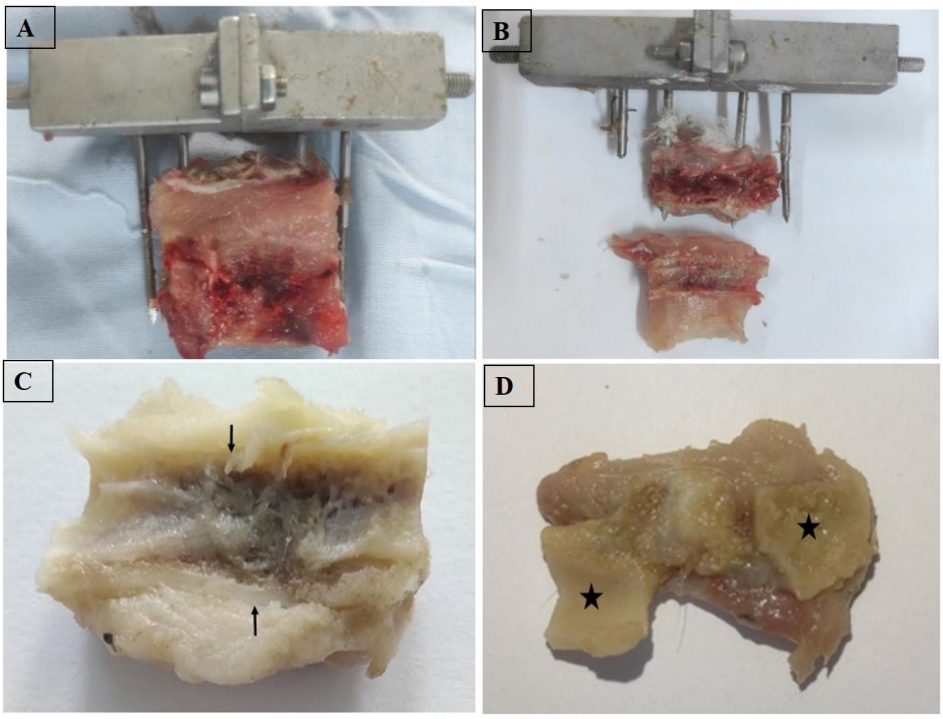

Figure 3. Post-euthanasia sample collection and macroscopic evaluation: **A**) En bloc resection of the bone and surrounding soft tissues between the two pins while preserving the external fixator; **B**) Longitudinal division of the resected block into two fragments; **C**) In the control group, macroscopic analysis showed complete cortical continuity restored (→) by a rigid bone bridge, with a homogeneous medullary cavity and no deformation; **D**) In the PS group, macroscopic evaluation revealed the absence of bone continuity restoration between the two bone ends (*) in a rabbit from the pseudarthrosis group.

radiological parameters assessed included cortical continuity, the appearance of the bone ends, the persistence of the interfragmentary gap, and the presence of bridging callus formation connecting the two bone ends.

Molecular analysis

To determine the expression of *COL1A1* and *RUNX2* during bone healing, the expression levels of COL1A1 mRNA and RUNX2 mRNA will be measured in two groups of healing tissues at the 8th week after the operation.

RNA extraction and cDNA synthesis

For RNA extraction, tissue from the shaft femoral fracture area was collected and immediately frozen in liquid nitrogen. The frozen tissue was ground to a fine powder in liquid nitrogen using a freezer mill (Bone Mill; SPEX CertiPrep, Metuchen, NJ, USA). TRIzol reagent (Invitrogen; Thermo Fisher Scientific, USA) was used to extract RNA from specimens according to the manufacturer's protocol followed by quantification with NanoDropND-1000 (Thermo Fisher Scientific). A quantity of 300 ng of RNA served as a template for complementary DNA (cDNA) synthesis using hexamer primers (50 nmol) and a dNTP mix (10 nmol). This step was followed by ten-minute incubation at 70°C. Next, buffer, DTT (0.2 µmol), and SuperScriptM II RTase (200 units) were added. The reaction was then incubated for 12 minutes at 25°C followed by 50 minutes at 42°C, and a final incubation at 70°C for 15 minutes.

Quantitative real-time PCR

Quantitative polymerase chain reaction: qPCR was performed using SYBR green master mix (Bio-Rad, USA). Primer sequences and annealing temperatures (Tm) are described in **Table 1**. The reaction was performed in a volume of 10 µl using the following protocol: denaturation at 95°C for five seconds, annealing at 58°C for 15 seconds, and extension at 72°C for 20 seconds, for 40 cycles. The relative amount of gene expression was calculated using the 2−ΔΔCt method, which was expressed by the mean (standard error). Experiments were performed in triplicate. The mean Ct values were calculated from triplicate PCRs for *RANKL*, *OPG*, *RUNX2*, and glyceraldehyde 3-phosphate dehydrogenase (*GAPDH*), and the ΔCt value for each specimen was obtained by subtracting these two values. Then the relative amount of *RANKL*, *OPG*, and *RUNX2* expressions were calculated by the 2−ΔΔCt method.

Table 1. Primer sequences and annealing temperature (T°).

COL1A1	Forward	5′ GCA ACA TGG AGA CTG GTG AG 3′
	Reverse	5′ GGA TGG AGG GAG TTT ACA GG 3′
Runx2 (cbfa1)	Forward	5′ CAG TGA TTT AGG GCG CAT TC 3′
	Reverse	5′ CTA GGC ACA TCG GTG AT G 3′
GADPH	Forward	5′ TCACCATCTTCCAGGAGCGA 3′
	Reverse	5′ CACAATGCCGAAGTGGTCGT 3′

Statistical analysis

Statistical analyses were performed using SPSS 20.0 (IBM, USA). Comparisons between two independent groups were carried out using the Mann–Whitney U test (Wilcoxon rank-sum test). A p-value <0.05 was considered statistically significant.

Results

Macroscopic and radiographic assessments of the shaft femoral pseudarthrosis rabbit model

For control group T, the macroscopic examination of the samples revealed that cortical continuity was reestablished by a rigid bone bridge in all rabbits. Furthermore, the medullary cavity appeared homogeneous, and no deformation was observed (**Figure 3C**).

In the other hand, in the second PS group, the macroscopic examination revealed the absence of reestablishment of bone continuity in all rabbits (**Figure 3D**). The tissue that united the two bone ends was heterogeneous in appearance and soft in consistency. Resorption of bone ends, indicated by widening of the resection gap and tapering or rounding of bone ends, was noted in all rabbits. No bone deformity was observed in any case.

The radiological analysis revealed a homogeneous and continuous callus, thick and continuous cortices, and a remodeled appearance of the bone with clear cortico-medullary differentiation for the control group. The emergence of ossification bridges and the early stages of bone remodeling and cortico-medullary differentiation were also observed (**Figure 4**). Overall, for all rabbits, a hard callus indicating radiological consolidation was evident after 8 weeks.

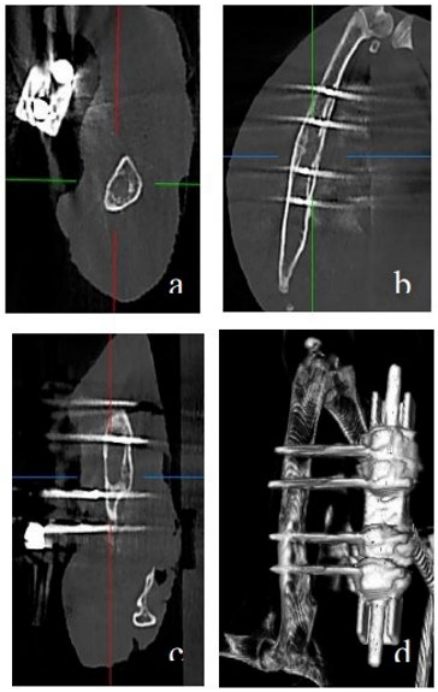

Figure 4. Radiological analysis in the control group showing a homogeneous and continuous callus, thick and continuous cortices, and a remodeled bone appearance with clear cortico-medullary differentiation. Early signs of ossification bridges and bone remodeling were also observed, **a**) axial, **b**) frontal, **c**) coronal sections and, **d**) in 3D reconstruction.

In the PS group, pseudarthrosis was observed in all cases. This was characterized by the presence of an interfragmentary gap, thin cortices interrupted at the resection site, a rounded and corticalized appearance of both bone ends, and occlusion of the medullary canal (**Figure 5**).

Molecular expression profiling of *RUNX2* and *COL1A1*

To compare the expression levels of the two genes between the two groups, their expression was quantified using qPCR.

RUNX2 gene expression

The expression levels of the *RUNX2* gene were analyzed in two groups: the control group (consolidation group) and the PS group. A significant difference in *RUNX2* gene expression between the two groups has been demonstrated ($p = 0.01$). As shown in **Figure 6A**, *RUNX2* expression was significantly higher in the control group compared to the PS group. The mRNA expression level of *RUNX2* in Group 2 (9.71 ± 4.65) was markedly higher than in Group 1 (0.97 ± 0.16), with a fold change of 10 (**Figure 6A**).

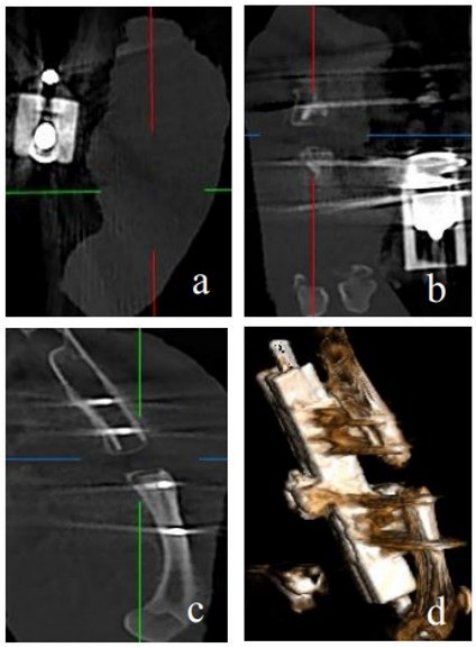

Figure 5. Radiological analysis in the PS group showing typical features of pseudarthrosis, including a persistent interfragmentary gap, thin and discontinuous cortices at the resection site, rounded and corticalized bone ends, and occlusion of the medullary canal. **a**) Axial, **b**) Frontal, **c**) Coronal sections, and **d**) 3D reconstruction.

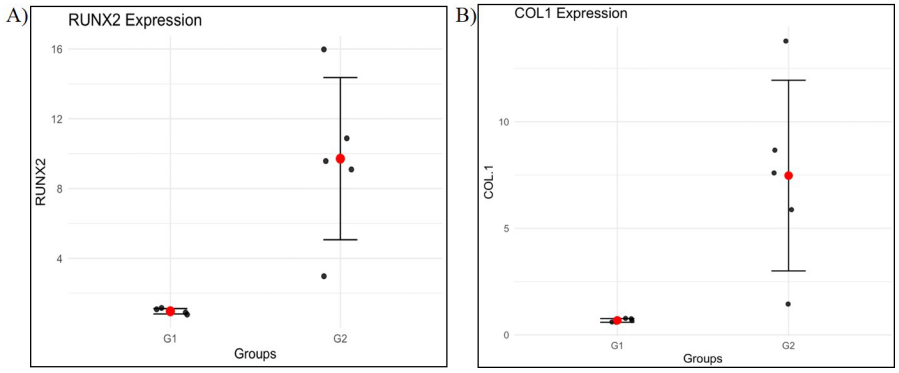

Figure 6. Expression of *COL1* and *Runx2* genes, **A**) Expression of the *Runx2* gene in the two groups (control group and PS group); **B**) Expression of the *COL1* gene in the two groups (control group and PS group).

COL1A1 gene expression

Similarly, the expression levels of the *COL1A1* gene were assessed in the same two groups and a significant difference in *COL1A1* gene expression has been demonstrated. As shown in **Figure 6B**, *COL1A1* expression was also significantly higher in the control group compared to the PS group ($p = 0.01$). The level of COL1 mRNA expression in PS group 2 (7,47380942± 4,47) is higher than group T (0,67930146 ± 0,08), with a fold change of 10 (**Figure 6B**).

Discussion

In this study, we aimed to develop a rabbit model of femoral shaft pseudarthrosis and to investigate the expression of *RUNX2* and *COL1A1* as a molecular approach to assess bone consolidation. For the first time, we successfully developed a rabbit model of femoral shaft pseudarthrosis, our model seems appropriate for studying the pathogenesis of PSA and testing new therapeutic approaches. Additionally, molecular outcomes validated this surgical technique through the analysis of *COL1A1* and *RUNX2* gene expression levels.

Within our study, we chose the rabbit as an animal model in accordance with the international guidelines for the care and management of laboratory animals. We considered the advantages of using rabbits, the availability of the necessary technical facilities, and, most importantly, the scarcity of pseudarthrosis models in this species. Additionally, in literature, rabbits are regarded as an ideal model for studies involving tissue engineering of cartilage, bone, tendons, and skin [22]. Moreover, the rabbit femur has been well-established as a model for osteological research since the 1980s [23,24].

We were interested in developing a pseudarthrosis model for several reasons. The high frequency of pseudarthrosis and the significant challenges it poses in the field of orthopedics. It is often associated with reduced bone quality. Moreover, treatment of pseudarthrosis remains challenging and subject to ongoing debate due to the variety of surgical techniques available and the lack of clearly defined indications [25].

As previously described, our technique is based on the interposition of the tensor fasciae latae (TFL) and represents a novel muscle interposition approach, described for the first time in a rabbit model. Several fixation techniques have been reported for the management of bone substance loss in animal models. In rabbits, internal fixation methods such as intramedullary nailing, centromedullary drilling, or screw–plate systems have been described [26,29]. In contrast, studies conducted in rat models which present distinct anatomical and biomechanical characteristics compared to rabbits have reported divergent findings. Gebauer *et al.* recommended intramedullary nailing for femoral bone substance loss in rats [30]. However, M. Jäger *et al.* demonstrated that intramedullary nailing may be inadequate for stabilizing bone substance defects, underscoring limitations that appear to be species-dependent and influenced by experimental conditions [31].

According to the literature, the external fixator is the most commonly used fixation system in bone healing studies requiring a high degree of stability [32,34]. For this reason, in our model, we opted for external fixation to ensure interfragmentary stability. We took care to secure the pins properly to prevent any spontaneous extraction, thereby maintaining the stability of the setup.

Regarding the size of the bone loss, numerous techniques have been described in the literature. According to Nauth *et al.*, there is no uniform definition of critical-size defects (CSD). However, in general, it refers to a bone defect that does not heal spontaneously despite surgical stabilization and requires additional surgical intervention, such as a bone autograft [35]. In the literature, a wide variety of definitions for CSD can be found, with different fixation systems. Most models developed in rats have chosen a CSD smaller than 10 mm. They have obtained a PSA in rats with small sizes of CSD [36].

In contrast, in our model, we chose a significant loss of substance of 10 mm and we obtained consolidation in the control group. This could be explained by the significant remodeling potential of the rabbit compared to the rat. Bone consolidation in the control group suggests that the size of the defect in our model has no influence on the creation of PSA.

The most commonly used techniques for creating a pseudarthrosis model in the literature include periosteal cauterization following diaphyseal resection of a long bone [37,41]. Additional, clinical and experimental evidence has shown that periosteal disruption at the fracture site can impair bone healing [42]. Kowalski *et al.* reported that the periosteum supplies blood to up to one-third of the cortical bone [43]. This highlights the importance of vascularization around the fracture site for normal healing and indicates that periosteal damage disrupts blood supply to the fracture site.

Other experimental techniques have been employed in the study of bone healing, including muscle interposition. In this context, Kumar *et al.* consider the interposition of soft tissues as a major factor in the development of pseudarthrosis, along with instability, infection, soft tissue injuries, and loss of vascularization [42].

In our model, we opted for the interposition of soft tissues at the osteotomy site. This element is essential to prevent bone healing. Suturing the TFL to the posterior thigh muscles using a Nylon thread, with a figure-eight configuration through the pins, provided better stability for the interposition. This approach effectively prevented its displacement during the

postoperative period. The choice of the TFL was based on several criteria. It is the most anterior muscle of the thigh, making it easily accessible. It is also a thin muscle, which facilitates its passage through the muscle compartments.

Ferreira *et al.* in 2009 established a similar pseudarthrosis model with regard to the choice of soft tissue interposition. However, this model differed in the choice of animal (rat) and the technique of fixing the TFL through two tunnels on either side of the fracture site [44]. In our study, we decided not to create these two tunnels to avoid weakening the femoral diaphysis and to prevent certain perioperative complications, such as the creation of bone defects or adjacent fractures.

The macroscopic and radiographic study showed, in control group T, a cortical continuity was reestablished by a rigid bone bridge in all rabbits, also, a hard callus indicating radiological consolidation was evident after 8 weeks. For the PS group, pseudarthrosis was oligotrophic, even atrophic, and resembled most animal models of pseudarthrosis. It was characterized by the presence of an interfragmentary gap, a rounded corticalized appearance at both ends, and occlusion of the medullary canal.

To validate our results, we opted for molecular biology study. We focused on the *COL1A1* gene, which encodes type I collagen, a key indicator of osteoid matrix production, and the *RUNX2* gene, responsible for the differentiation of stem cells into the osteoblastic lineage. These two genes have a crucial role in bone formation. Indeed, *RUNX2* is a key transcription factor essential for the differentiation of mesenchymal stem cells into osteoblasts, the cells responsible for bone formation. It regulates the expression of several osteogenic genes, including *COL1A1*, which encodes type I collagen, the primary structural protein of the bone matrix. Together, *RUNX2* and *COL1A1* play pivotal roles in promoting osteoblast activity and ensuring proper bone formation and mineralization [45].

Our results revealed the high expression levels of *RUNX2* and *COL1A1* genes were significantly higher in the control group compared to the PS group. These results confirmed macroscopic and radiographic results. Bone healing was assessed through macroscopic, radiological, and molecular analyses.

Conclusion

The analysis of the results demonstrated clear radiological and anatomopathological consolidation in all rabbits from the control group, accompanied by robust expression of the *COL1A1* and *RUNX2* genes. In contrast, the PS group exhibited pseudarthrosis. This condition was confirmed by macroscopic, radiographic, and molecular analyses. Notably, the PS group showed significantly reduced expression levels of the *COLIA1* and *Runx2* genes, suggesting that their downregulation could serve as a critical biomarker for pseudarthrosis in future studies.

In conclusion, we successfully developed, for the first time, a femoral pseudarthrosis model in rabbits. This model is highly reproducible and provides a valuable experimental platform for investigating the mechanisms of bone healing and exploring innovative therapeutic approaches for treating pseudarthrosis.

Conflict of interest

All authors declare that there is no conflict of interest.

Funding

This research did not receive any specific Grant from funding agencies in the public, commercial, or not-for-profit sectors.

Acknowledgments

This work was funded by the Tunisian Ministry of Higher Education and Scientific Research. The authors thank the patients and their families for their cooperation in the present study.

References

1. Basile G, Avato FM, Passeri A, Accetta R, Amadei F, Giorgetti A, et al. Atrophic pseudarthrosis of humeral diaphyseal fractures: medico-legal implications and methodological analysis of the evaluation. Acta Biomed. 2022 Jul 1;93(3):e2022176.
2. Lambiris E, Panagopoulos A, Zouboulis P, Sourgiadaki E. Current Concepts: Aseptic Nonunion of Femoral Shaft Diaphysis. Eur J Trauma Emerg Surg. 2007 Apr;33(2):120–34.
3. Bianco Prevot L, Nannini A, Mangiavini L, Bobba A, Buzzi S, Sinigaglia F, et al. What Is the Best Treatment of the Femoral Shaft Nonunion after Intramedullary Nailing? A Systematic Review. Life (Basel). 2023 Jul 4;13(7):1508.
4. Gómez-Barrena E, Padilla-Eguiluz NG, Rosset P. Frontiers in non-union research. EFORT Open Rev. 2020 Oct 26;5(10):574–83.
5. Ekegren CL, Edwards ER, de Steiger R, Gabbe BJ. Incidence, Costs and Predictors of Non-Union, Delayed Union and Mal-Union Following Long Bone Fracture. Int J Environ Res Public Health. 2018 Dec 13;15(12):2845.
6. Basile G, Avato FM, Passeri A, Accetta R, Amadei F, Giorgetti A, et al. Atrophic pseudarthrosis of humeral diaphyseal fractures: medico-legal implications and methodological analysis of the evaluation. Acta Biomed. 2022 Jul 1;93(3):e2022176.
7. Yang J, Zhang X, Liang W, Chen G, Ma Y, Zhou Y, et al. Efficacy of adjuvant treatment for fracture nonunion/delayed union: a network meta-analysis of randomized controlled trials. BMC Musculoskelet Disord. 2022 May 21;23(1):481.

8. Auersperg V, Trieb K. Extracorporeal shock wave therapy: an update. EFORT Open Rev. 2020 Oct 26;5(10):584–92.

9. Sansone V, Ravier D, Pascale V, Applefield R, Del Fabbro M, Martinelli N. Extracorporeal Shockwave Therapy in the Treatment of Nonunion in Long Bones: A Systematic Review and Meta-Analysis. J Clin Med. 2022 Apr 1;11(7):1977.

10. Rupp M, Biehl C, Budak M, Thormann U, Heiss C, Alt V. Diaphyseal long bone nonunions - types, aetiology, economics, and treatment recommendations. Int Orthop. 2018 Feb;42(2):247–58.

11. Wu S, Quan K, Mei J, Dai M, Song S. Cortical allograft strut augmented with platelet-rich plasma for the treatment of long bone non-union in lower limb- a pilot study. BMC Musculoskelet Disord. 2022 May 30;23(1):512.

12. Attum B, Douleh D, Whiting PS, White-Dzuro GA, Dodd AC, Shen MS, et al. Outcomes of Distal Femur Nonunions Treated With a Combined Nail/Plate Construct and Autogenous Bone Grafting. J Orthop Trauma. 2017 Sep;31(9):e301–4.

13. Perisano C, Cianni L, Polichetti C, Cannella A, Mosca M, Caravelli S, et al. Plate Augmentation in Aseptic Femoral Shaft Nonunion after Intramedullary Nailing: A Literature Review. Bioengineering (Basel). 2022 Oct 16;9(10):560.

14. Hierholzer C, Friederichs J, Glowalla C, Woltmann A, Bühren V, von Rüden C. Reamed intramedullary exchange nailing in the operative treatment of aseptic tibial shaft nonunion. Int Orthop. 2017 Aug;41(8):1647–53.

15. O'Halloran K, Coale M, Costales T, Zerhusen T Jr, Castillo RC, Nascone JW, et al. Will My Tibial Fracture Heal? Predicting Nonunion at the Time of Definitive Fixation Based on Commonly Available Variables. Clin Orthop Relat Res. 2016 Jun;474(6):1385–95.

16. Onishi T, Shimizu T, Akahane M, Okuda A, Kira T, Omokawa S, et al. Robust method to create a standardized and reproducible atrophic non-union model in a rat femur. Journal of Orthopaedics. 2020;21:223–7.

17. Schindeler A, Morse A, Harry L, Godfrey C, Mikulec K, McDonald M, et al. Models of tibial fracture healing in normal and Nf1-deficient mice. J Orthop Res. 2008 Aug;26(8):1053–60.

18. Smirnov SS, Shchepkina EA, Shilenko LA, Samsonenko EK, Anikin NA, Mametov MV, et al. Experimental model of normotrophic pseudarthrosis of a rabbit's tibia. Acta Biomedica Scientifica. 2022 Dec 11;7(5-2):268-79.

19. Lian JB, Stein GS. Runx2/Cbfa1: a multifunctional regulator of bone formation. Curr Pharm Des. 2003;9(32):2677–85.

20. Selvaraj V, Sekaran S, Dhanasekaran A, Warrier S. Type 1 collagen: Synthesis, structure and key functions in bone mineralization. Differentiation. 2024 Mar-Apr;136:100757.

21. Iacobellis C, Cacciato F. Aseptic nonunion and delay in consolidation in the tibia: treatment by intramedullary nailing and using the Ilizarov method. Chir Organi Mov. 2001 Jul-Sep;86(3):199–210.

22. Lapi S, Nocchi F, Lamanna R, Passeri S, Iorio M, Paolicchi A, et al. Different media and supplements modulate the clonogenic and expansion properties of rabbit bone marrow mesenchymal stem cells. BMC Res Notes. 2008 Jul 28;1:53.

23. Concannon MJ, Boschert MT, Puckett CL. Bone induction using demineralized bone in the rabbit femur: a long-term study. Plast Reconstr Surg. 1997 Jun;99(7):1983–8.

24. Weissman SL, Tadmor A, Khermosh O, Michels CH, Chen R. Growth of the upper end of the femur. Experimental investigation in the rabbit. Acta Orthop Scand. 1974;45(2):225–34.

25. Basile G, Fozzato S, Petrucci QA, Gallina M, Bianco Prevot L, Accetta R, et al. Treatment of Femoral Shaft Pseudarthrosis, Case Series and Medico-Legal Implications. J Clin Med. 2022 Dec 14;11(24):7407.

26. Crigel MH, Balligand M. Critical size defect model on the femur in rabbits. Veterinary and Comparative Orthopaedics and Traumatology. 2002;15(03):158–63.

27. Onishi T, Shimizu T, Akahane M, Okuda A, Kira T, Omokawa S, et al. Robust method to create a standardized and reproducible atrophic non-union model in a rat femur. J Orthop. 2020 Mar 28;21:223–7.

28. Garcia P, Holstein JH, Maier S, Schaumlöffel H, Al-Marrawi F, Hannig M, et al. Development of a reliable non-union model in mice. J Surg Res. 2008 Jun 1;147(1):84–91.

29. Oetgen ME, Merrell GA, Troiano NW, Horowitz MC, Kacena MA. Development of a femoral non-union model in the mouse. Injury. 2008 Oct;39(10):1119–26.

30. Gebauer GP, Lin SS, Beam HA, Vieira P, Parsons JR. Low-intensity pulsed ultrasound increases the fracture callus strength in diabetic BB Wistar rats but does not affect cellular proliferation. J Orthop Res. 2002 May;20(3):587–92.

31. Jäger M, Sager M, Lensing-Höhn S, Krauspe R. The critical size bony defect in a small animal for bone healing studies (II): Implant evolution and surgical technique on a rat's femur/ Der kritische Knochendefekt am Kleintier zur Untersuchung der Knochenheilung (II): Implantatentwicklung und Operationstechnik am Rattenfemur.

32. Harrison LJ, Cunningham JL, Strömberg L, Goodship AE. Controlled induction of a pseudarthrosis: a study using a rodent model. J Orthop Trauma. 2003 Jan;17(1):11–21.

33. Mark H, Bergholm J, Nilsson A, Rydevik B, Strömberg L. An external fixation method and device to study fracture healing in rats. Acta Orthop Scand. 2003 Aug;74(4):476–82.

34. Moore DC, Pedrozo HA, Crisco JJ 3rd, Ehrlich MG. Preformed grafts of porcine small intestine submucosa (SIS) for bridging segmental bone defects. J Biomed Mater Res A. 2004 May 1;69(2):259–66.

35. Nauth A, Schemitsch E, Norris B, Nollin Z, Watson JT. Critical-Size Bone Defects: Is There a Consensus for Diagnosis and Treatment? J Orthop Trauma. 2018 Mar;32 Suppl 1:S7–11.

36. Kokubu T, Hak DJ, Hazelwood SJ, Reddi AH. Development of an atrophic nonunion model and comparison to a closed healing fracture in rat femur. J Orthop Res. 2003 May;21(3):503–10.

37. Hietaniemi K, Peltonen J, Paavolainen P. An experimental model for non-union in rats. Injury. 1995 Dec;26(10):681–6.

38. Garcia P, Histing T, Holstein JH, Klein M, Laschke MW, Matthys R, et al. Rodent animal models of delayed bone healing and non-union formation: a comprehensive review. Eur Cell Mater. 2013 Jul 16;26:1-12; discussion 12–4.

39. Kaspar K, Matziolis G, Strube P, Sentürk U, Dormann S, Bail HJ, et al. A new animal model for bone atrophic nonunion: fixation by external fixator. J Orthop Res. 2008 Dec;26(12):1649–55.

40. Wu XQ, Wang D, Liu Y, Zhou JL. Development of a tibial experimental non-union model in rats. J Orthop Surg Res. 2021 Apr 14;16(1):261.

41. Kumar G, Narayan B. The biology of fracture healing in long bones. In: Classic Papers in Orthopaedics. London: Springer London; 2013. pp. 531–3.

42. Kowalski MJ, Schemitsch EH, Kregor PJ, Senft D, Swiontkowski MF. Effect of periosteal stripping on cortical bone perfusion: a laser doppler study in sheep. Calcif Tissue Int. 1996 Jul;59(1):24–6.

43. Ferreira ML, Silva PC, Pereira Lde P, Franco RS, Mello NB, Amaral AC, et al. Modelo experimental em ratos para o desenvolvimento de pseudoartrose [Experimental model in rats for the development of pseudoarthrosis]. Rev Col Bras Cir. 2009 Dec;36(6):514–8.

44. Heo SK, Choi Y, Jeong YK, Ju LJ, Yu HM, Kim DK, et al. LIGHT (TNFSF14) enhances osteogenesis of human bone marrow-derived mesenchymal stem cells. PLoS One. 2021 Feb 19;16(2):e0247368.